Analysis of Immunogenic Galactose-alpha-1,3-galactose-Containing N-Glycans in beef, mutton, and pork tenderloin by Combining Matrix-Assisted Laser Desorption/Ionization-mass spectroscopy and capillary electrophoresis hyphenated with mass spectrometry via electrospray ionization

Guo, R.R.; Lageveen-Kammeijer, G.S.M.; Wang, W.J.; Dalebout, H.; Zhang, W.A.; Wuhrer, M.; ... ; Voglmeir, J.

JOURNAL OF AGRICULTURAL AND FOOD CHEMISTRY

pubs.acs.org/JAFC

Article

Analysis of Immunogenic Galactose-α-1,3-galactose-Containing *N*-Glycans in Beef, Mutton, and Pork Tenderloin by Combining Matrix-Assisted Laser Desorption/Ionization-Mass Spectroscopy and Capillary Electrophoresis Hyphenated with Mass Spectrometry via Electrospray Ionization

Rui-Rui Guo, Guinevere S. M. Lageveen-Kammeijer, Wenjun Wang, Hans Dalebout, Wangang Zhang, Manfred Wuhrer, Li Liu,* Bram Heijs,* and Josef Voglmeir*

Cite This: *J. Agric. Food Chem.* 2023, 71, 4184−4192

Read Online

ACCESS | Metrics & More | Article Recommendations | Supporting Information

ABSTRACT: Severe allergic reactions to certain types of meat following tick bites have been reported in geographic regions which are endemic with ticks. This immune response is directed to a carbohydrate antigen (galactose-α-1,3-galactose or α-Gal), which is present in glycoproteins of mammalian meats. At the moment, asparagine-linked complex carbohydrates (*N*-glycans) with α-Gal motifs in meat glycoproteins and in which cell types or tissue morphologies these α-Gal moieties are present in mammalian meats are still unclear. In this study, we analyzed α-Gal-containing *N*-glycans in beef, mutton, and pork tenderloin and provided for the first time the spatial distribution of these types of *N*-glycans in various meat samples. Terminal α-Gal-modified *N*-glycans were found to be highly abundant in all analyzed samples (55, 45, and 36% of *N*-glycome in beef, mutton, and pork, respectively). Visualizations of the *N*-glycans with α-Gal modification revealed that this motif was mainly present in the fibroconnective tissue. To conclude, this study contributes to a better understanding of the glycosylation biology of meat samples and provides guidance for processed meat products, in which only meat fibers are required as an ingredient (i.e., sausages or canned meat).

KEYWORDS: *galactose-α-1,3-galactose, N-glycans, meat allergens, MALDI-TOF-MS, mass spectrometry imaging*

INTRODUCTION

Human allergic reactions against red meat (i.e., beef, mutton, or pork) following tick bites (Figure 1a) were first reported in 2009 by van Nunen and co-workers.[1] Since then, different groups have further investigated this phenomenon for various geographical regions with endemic tick populations and reported similar results to the 2009 study (Australia,[2,3] Europe,[4] and America[5]). It was subsequently revealed that these allergic reactions to red meat are triggered by immunoglobulin E (IgE)-sensitized mast cells and, more specifically, to a post-translational carbohydrate modification of the meat proteins, namely, the *N*-glycan-linked galactose-α-1,3-galactose (α-Gal) motif.[6−9] This α-Gal motif is omnipresent in all mammals except humans and Old World monkeys[7] and results from the α-1,3-galactosyltransferase (α1,3GT)-mediated addition of a terminal galactose residue to the galactose of complex *N*-glycans in α-1,3-linkage which takes place in the Golgi apparatus.[10−12] In contrast to most other mammals, humans are unable to synthesize the α-Gal motif due to two-point mutations in the α1,3-galactosyltransferase gene coding for α1,3GT and making it catalytically inactive.[13−15] This particular α-Gal carbohydrate motif has since also been identified in the saliva of ticks. Upon a tick bite, saliva containing α-Gal-decorated *N*-glycans enters the human skin and triggers an IgE antibody-directed hypersensitivity against α-Gal.[16−18]

Prior to the exposure to the α-Gal motif via tick bites, patients with red meat allergy were able to consume red meat on a regular basis (1−2 times a week) for years without any noticeable symptoms.[5] The described allergic symptoms include itching and swelling of the skin and, in some cases, severe anaphylaxis was reported.[19,20] Interestingly, in comparison to the rapid onset period of under 2 hours of other known IgE-induced food allergies, red meat-induced allergic reactions generally require a longer onset period of 3 to 6 hours.[18] Diary glycoproteins are digested into small molecules (e.g., amino acids and small molecular weight peptides), ensuring that the nutrients could be absorbed by the intestine.[21,22] In addition, the stability of glycoproteins may be also affected in a gastrointestinal environment,[23] with nonhuman glycan motifs increasing the resistance of glycoprotein digestion.[21,24] Therefore, it is hypothesized that this delayed immune response is caused by slower proteolytic degradation of α-Gal-bearing meat glycoproteins prior to their absorption into the circulatory system.[25]

Received: November 19, 2022
Revised: February 2, 2023
Accepted: February 7, 2023
Published: February 21, 2023

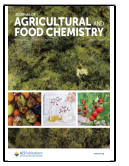

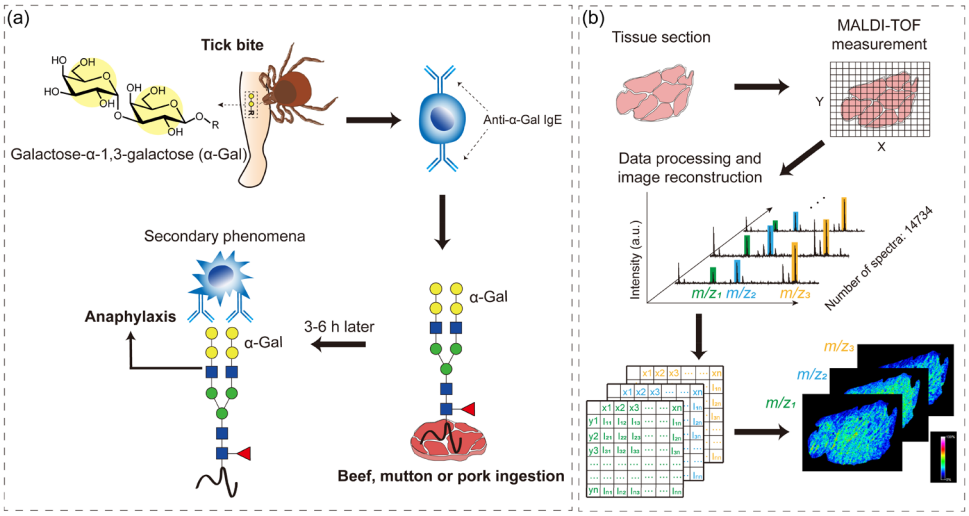

Figure 1. (a) Development of allergic reactions after tick bites to the α-Gal motif in meats and (b) overview on the spatial distribution of analytes using MSI.

While the role of α-Gal sensitization in mammalian meat allergy has thoroughly been investigated and demonstrated as illustrated above, the α-Gal moiety, as the terminal modification linked to *N*-glycans, has been rarely investigated in meat samples until now. Furthermore, protein glycosylation in meat samples is so far only studied using homogenized tissues.[26,27] Matrix-assisted laser desorption/ionization mass spectrometry imaging (MALDI-MSI) allows one to address this by generating two-dimensional illustrations of selected analytes by scanning the surface of biological samples (Figure 1b).[28−30] This methodology is generally used to detect analytes such as proteins,[31] peptides,[32] lipids,[33] and metabolites,[34] but various studies also report on its usage to explore the distribution of the *N*-glycome.[35−40] While MALDI-MSI has already been applied in food studies,[41,42] this technique has, to the best of our knowledge, not yet been exploited to investigate the *N*-glycome distribution of various meats. Therefore, the identity and spatial distribution of α-Gal-containing *N*-glycans in meat species is of keen interest from the nutritional perspective and consequently can provide scientific guidance for meat manufacturing, especially for processed meat products. We herein analyzed the homogeneous and spatial distribution of the responsible α-Gal motif of the *N*-glycans in beef, mutton, and pork tenderloin by a combination of MALDI-TOF-MS, capillary electrophoresis hyphenated with mass spectrometry via electrospray ionization CE-ESI-MS(/MS), and MALDI-MSI. By this approach, the abundance of *N*-glycans with α-Gal motif in different tenderloin samples could be analyzed both at an in-depth and at the spatial level.

MATERIALS AND METHODS

Materials. Glacial acetic acid (HAc) and ethanol (EtOH) were obtained from Merck (Darmstadt, Germany). Formaldehyde solution (4%) (buffered, pH 6.9), 40% dimethylamine, dimethylsulfoxide (DMSO), 28% ammonium hydroxide solution, 1-hydroxybenzotriazole hydrate (HoBt), α-cyano-4-hydroxycinnamic acid (CHCA), trifluoroacetic acid (TFA), trichloroacetic acid, poly-L-lysine 0.1% solution, Nonidet P-40 substitute, and maltoheptaose (DP7) were purchased from Sigma-Aldrich (St. Louis, MO, USA). 1-Ethyl-3-(3-dimethylaminopropyl)carbodiimide (EDC) was obtained from Fluorochem (Hadfield, UK). HPLC SupraGradient acetonitrile (ACN) was purchased from Biosolve (Valkenswaard, The Netherlands). Recombinant PNGase F PRIME-LY glycosidase from *Flavobacterium meningosepticum* was purchased from N-Zyme Scientifics (Doylestown, PA, USA). 1-(Hydrazinocarbonylmethyl)-pyridinium chloride (Girard's Reagent P; GirP; cat. nr. G0030) was purchased from TCI Development Co. Ltd. (Tokyo, Japan). Indium-tin-oxide (ITO) glass slides and peptide calibration standard II were purchased from Bruker Daltonics (Bremen, Germany). All buffers were prepared using deionized water generated from a Q-card 2 system (Millipore).

Meat Sample Preparation. Three dry-aged meat samples for each species (beef, mutton, and pork), which were representative for the Dutch consumer market, were purchased from a butcher in Leiden, the Netherlands. Ice cold phosphate buffered saline (1 × PBS) was used to remove excessive tissue fluids. For the determination of the homogenous *N*-glycan composition, approximately 100 mg of each meat sample was frozen in liquid nitrogen and homogenized with a mortar and pestle. For the spatial *N*-glycan release, each meat sample was cut into roughly 10 mm × 5 mm × 2 mm blocks. For the purpose of tissue fixation, the meat samples were further incubated in 4% formaldehyde solution (v/v, pH 6.9, the ratio of fixative volume to tissue volume is 10:1) at room temperature for 24 h to protect tissues from post-mortem degradation and to prevent protein delocalization during further tissue processing. The formalin-fixed tissue blocks were then cut into 10 μm thick slices and mounted on poly-L-lysine and indium-tin-oxide (ITO)-coated glass slides. The slices were dried in a vacuum desiccator for 10 min and stored at −80 °C for further analysis.

***N*-Glycan Release.** The release of *N*-glycans was performed as previously described.[26] In brief, approximately 100 mg of minced meat was suspended in 500 μL of deionized water, followed by the addition of 500 μL of 40% trichloroacetic acid (TCA, v/v) for protein precipitation. After centrifugation at 12,000 × *g* for 10 min, the supernatant was removed. The obtained proteins were washed with deionized water until the supernatant of the suspension was pH neutral. The proteins were resuspended in 400 μL of deionized water. The resulting protein solution was only denatured by heating (95 °C for 10 min); no denaturing agents (such as dithiothreitol or sodium dodecyl sulfate) were used to avoid interference with the subsequent linkage-specific derivatization procedures. A total of 10 μL of PNGase F (0.2 mg/mL) was added after the sample cooled down to room temperature. The enzymatic *N*-glycan release was performed at 37 °C overnight. The released *N*-glycans were collected by centrifugation at 12,000 × *g* for 10 min followed by centrifugal evaporation to concentrate the sample to a volume of 10 μL. The concentrated *N*-

https://doi.org/10.1021/acs.jafc.2c08067
J. Agric. Food Chem. 2023, 71, 4184−4192

glycans were directly used for sialic acid ethyl esterification and amidation.

Sialic Acid Ethyl Esterification and Amidation. Linkage-specific derivatization of sialic acids through ethyl esterification of α2,6-linked sialic acid residues and via amide formation of α2,3-linked sialic acids was performed as previously described.[43] Briefly, 1 μL of concentrated meat *N*-glycans was added to 20 μL of ethyl esterification reagent (0.25 M EDC and 0.25 M HoBt in EtOH) and incubated at 37 °C for 30 min. After the addition of 4 μL of 28% NH_4OH, an additional incubation was followed for 30 min at 37 °C. Afterward, 24 μL of ACN was added, and the *N*-glycans were isolated by cotton HILIC (hydrophilic interaction liquid chromatography) solid phase extraction, as previously described.[44] In short, a 3−4 mm long cotton thread was positioned at the bottom of 20 μL tips. The cotton was conditioned three times with 10 μL of deionized water and subsequently equilibrated three times with 85% ACN. The sample was loaded onto the cotton by slowly aspirating and dispensing the sample with the pipette twenty times, followed by a washing step with 85% aqueous ACN containing 1% TFA and a second washing step with 85% aqueous ACN. The *N*-glycans were eluted by aspirating and dispensing the sample for five times in 10 μL of deionized water.

MALDI-TOF-MS Measurement and Data Processing. For MALDI analysis, 5 μL of purified *N*-glycan sample was spotted on an Anchorchip 384 MALDI plate (Bruker Daltonics, Bremen, Germany) and overlayed with 1 μL of DHB matrix solution (5 mg/mL with 1 mM NaOH in 50% ACN). Mass spectra were recorded from m/z 900 to 4500 using a rapifleX MALDI-TOF mass spectrometer (Bruker Daltonics) in positive ion reflectron mode. For every spectrum, 10,000 laser shots were summed and recorded using a random walk pattern at a repetition rate of 1000 Hz. Per raster spot 500 shots were used. Mass spectra were processed with flexAnalysis software (Version 3.4 Build 50, Bruker Daltonics) and further analyzed with the MassyTools glycan processing software,[45] which standardized the calibration of mass spectra and performed quality control calculations based on a user-defined list of glycans. The following selection criteria were chosen: <20 ppm mass error, S/N ratio > 9, isotopic pattern quality (IPQ) score > ±0.2 score. The *N*-glycan relative abundances are fractions of the total signal (100%). The workflow for the MALDI-TOF-MS measurement of beef, mutton, and pork tenderloin *N*-glycans analysis is shown in Supporting Information, Figure S1a.

CE-ESI-MS/MS Measurement and Data Processing. The 10 μL sample containing derivatized and purified *N*-glycans solutions were dried by centrifugal evaporation. Subsequently, 2 μL of GirP reagent (50 mM GirP in 90% EtOH and 10% HAc) was added for labeling (the working principle is shown in the Supporting Information, Figure S1b). All experiments were performed on a bare fused capillary cartridge (90 cm long, 30 μm ID, 150 μm OD, SCIEX Framingham, MA, USA) using a CESI 8000 system (Sciex, Framingham, MA, USA). Prior to each analysis, the capillary was rinsed thoroughly with 0.1 M NaOH (2.5 min), 0.1 M HCl (2.5 min), ultrapure water (4 min), and the background electrolyte (BGE) of 20% HAc (4 min) at 100 psi. The conductive line was rinsed with BGE for 3 min at 75 psi. Before analysis, all samples were diluted with the leading electrolyte (ammonium acetate at pH 3.17, final concentration 400 mM). Injection of the samples was performed hydrodynamically by applying 25 psi for 24 s (corresponding to 14% of the total capillary volume ~88 nL), unless stated otherwise. After each sample injection, a BGE post plug was injected by applying 0.5 psi for 25 s (0.3% of the capillary volume). For each analysis, a constant flow was established, by applying 2 psi and 20 kV over the capillary with a constant temperature of 20 °C.

The CESI 8000 system was coupled to an Impact HD UHR-QqTOF-MS (Bruker Daltonics) via a sheathless CE-ESI-MS interface (Sciex) which allowed alignment between the capillary spray tip and the front of the nanospray shield (Bruker Daltonics). All experiments with DEN-gas were performed in positive ionization mode with a capillary voltage of 1200 V. In addition, an in-house made polymer cone was attached onto the porous tip housing to enable the usage of the DEN-gas.[46] For all analysis, the temperature and flow rate of the drying gas were set at 150 °C and 1.2 L/min, respectively. To minimize the in-source decay, the collision cell energy as well as the quadrupole ion energy were set at 7.0 eV and the pre-pulse storage was set at 15.0 μs. The theoretical masses highlighted with yellow color were used for targeted CE-ESI-MS/MS analysis (see the Supporting Information, Table S1−S3). Depending on the m/z values, the precursor ions were isolated with a width of 8, 10, 15, or 15 Th at m/z 500, 800, 1300, 1500, respectively. The collision energies were set as a linear curve in a m/z-dependent manner, ranging from 20 eV at m/z 150 to 70 eV at m/z 3500 for all charge states (1−3), applying a basic stepping mode with collision energies of 100% (80% of the time) or 50% (20% of the time). Acquired mass spectra were processed using the DataAnalysis software package (Version 5.0 Build 203.2.3586, Bruker Daltonics). The workflow for the CE-ESI-MS measurement of beef, mutton, and pork tenderloin *N*-glycans analysis is shown in the Supporting Information, Figure S1a.

In Situ Derivatization and *N*-Glycan Release. Tissue sections were transferred to the center part of the ITO glass slides and conditioned using sequential solvent washes in 100% EtOH (10 × 2 s), 70% EtOH (10 × 2 s), 50% EtOH (10 × 2 s) and deionized water (10 × 2 s). Afterward, the slides were dried in a vacuum desiccator for 10 min. Linkage-specific sialic acid derivatization as well as the *N*-glycan release were carried out as described before.[47] Briefly, tissue slides were incubated in derivatization solution (0.25 M EDC, 0.5 M HoBt, and 0.25 M dimethylamine in DMSO) at 60 °C for 1 h, and additional incubation for 2 h at 60 °C was followed after the addition of 28% NH_4OH (the ratio of derivatization solution to 28% ammonia solution is 1:0.4 (v/v)). The tissue sections were rinsed with 50 mL of EtOH after derivatization and sequentially washed with EtOH (2 × 2 min) and deionized water (2 × 5 min). Sample slides were dried in a vacuum desiccator for 10 min before PNGase F solution (0.2 mg/mL in water) was sprayed homogeneously on a tissue slide using a SunCollect spraying robot (Sunchrom, Friedrichsdorf, Germany) applying 10 layers at 10 μL/min with the following settings: 1 mm of line distance, 30 mm of motor height (Z direction), and 900 mm/min of motor speeds (X and Y directions). The *N*-glycans were released at 37 °C for 16 h in a humid environment. After incubation, the slides were dried in a vacuum desiccator for 10 min, and the MALDI matrix including a maltoheptaose DP7 internal standard (0.25 μM DP7 in 50% ACN containing 5 mg/mL CHCA) was applied in 6 layers using the SunCollect spraying robot (layer 1: 10 μL/min, layer 2: 20 μL/min, layer 3: 30 μL/min, layer 4−6: 40 μL/min) with settings of 2 mm line distance, 25 mm motor height, and 900 mm/min motor speeds. Using CHCA and this layered matrix application scheme resulted in smaller crystal growth compared to the DHB matrix and allowed a higher spatial resolution during MALDI-MSI analysis. The sprays of PNGase F solution and the MALDI matrix were both performed under 30 psi of nitrogen pressure.

MALDI-MSI Measurement and Data Analysis. The MALDI-MSI measurement of *N*-glycans was performed using a rapifleX MALDI-TOF/TOF instrument (Bruker Daltonics) in positive ion reflectron mode. Mass spectra were recorded from m/z 900 to 4500 using 1000 laser shots per pixel with 50 × 50 pixel size (laser setting "single"). MSI data acquisition was enabled by the flex-software suite (flexImaging 5.0 Build 80, flexControl 4.0 Build 46). MSI data were normalized to the total ion count (TIC) using the flexImaging software package (Version 5.0 Build 80, Bruker Daltonics). The selected peaks were monoisotopic masses and the mass range was set to m/z ± 0.01%. The glycan annotation was performed in GlycoWorkbench (Version 1.1 Build 3480). The workflow scheme for the MALDI-MSI measurement of the beef, mutton, and pork tenderloin *N*-glycans analysis is shown in the Supporting Information, Figure S2.

RESULTS

N-Glycan Analyses of Meats in Homogenous Tissues.

The analysis of protein-linked carbohydrates using MALDI-TOF-MS can result in ionization biases due to the lability of sialic acid modifications.[47] Therefore, sialic acids were neutralized and stabilized by chemical derivatization after the

https://doi.org/10.1021/acs.jafc.2c08067
J. Agric. Food Chem. 2023, 71, 4184−4192

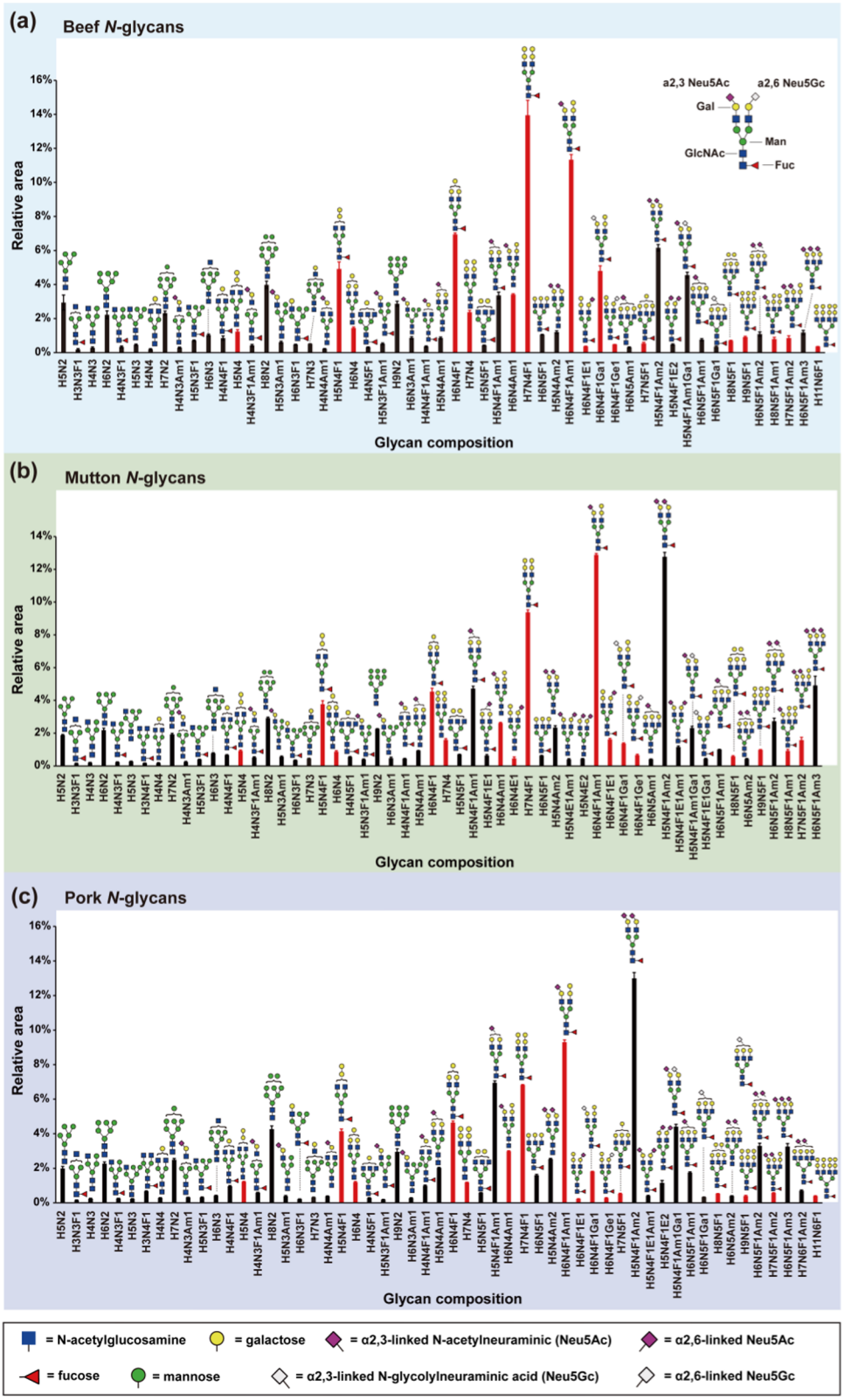

Figure 2. MALDI-TOF-MS *N*-glycan profiles obtained from (a) beef, (b) mutton, and (c) pork. The glycan compositions are shown. Error bars represent the standard deviation (n = 3); the replicated relative abundances of glycan compositions from beef, mutton, and pork are, respectively, shown in the Supporting Information, Tables S1−S3. The red columns represent *N*-glycans with the terminal α-Gal motif; the black columns represent *N*-glycans without the α-Gal motif. H = hexose, N = *N*-acetylhexosamine, F = fucose, Am = amidated *N*-acetylneuraminic acid (α2,3-linked Neu5Ac), E = ethyl esterified *N*-acetylneuraminic acid (α2,6-linked Neu5Ac), Ga = amidated *N*-glycolylneuraminic acid (α2,3-linked Neu5Gc), and Ge = ethyl esterified *N*-glycolylneuraminic acid (α2,6-linked Neu5Gc).

https://doi.org/10.1021/acs.jafc.2c08067
J. Agric. Food Chem. 2023, 71, 4184−4192

enzymatic *N*-glycan release by PNGase F and analyzed by MALDI-TOF-MS and CE-ESI-MS (Supporting Information, Table S1−S3). Extracted ion electropherograms of several typical *N*-glycans from beef, mutton, and pork tenderloin are shown in the Supporting Information, Figure S3. CE-ESI-MS(/MS) of *N*-glycans after GirP labeling was used to further elucidate glycan compositions from each meat sample (Supporting Information, Figures S4−S6). The stable cationic character of this derivatization agent allows an efficient mass spectrometric analysis of the *N*-glycans.[43,48] In total, 53, 56, and 55 *N*-glycans were identified in beef, mutton, and pork, respectively (Supporting Information, Figures S7−S9 and Table S1−S3). The identity and abundance of meat *N*-glycans based on the obtained MALDI-TOF mass spectra are summarized in Figure 2. The α-Gal motif was present on multiple *N*-glycan structures (a total of 17, 16, and 16 *N*-glycan species in beef, mutton, and pork, respectively). Detected *N*-glycans were classified into six structural groups: oligomannosidic type, *N*-glycans with the terminal α-Gal motif (consists of only terminal α-Gal, both terminal α-Gal and *N*-acetylneuraminic (Neu5Ac) or *N*-glycolylneuraminic acid (Neu5Gc)), Neu5Ac or Neu5Gc motif, *N*-glycans with both terminal Neu5Ac and Neu5Gc motifs, and neutral complex *N*-glycans without α-Gal motif (Figure 3). The relative abundances of the

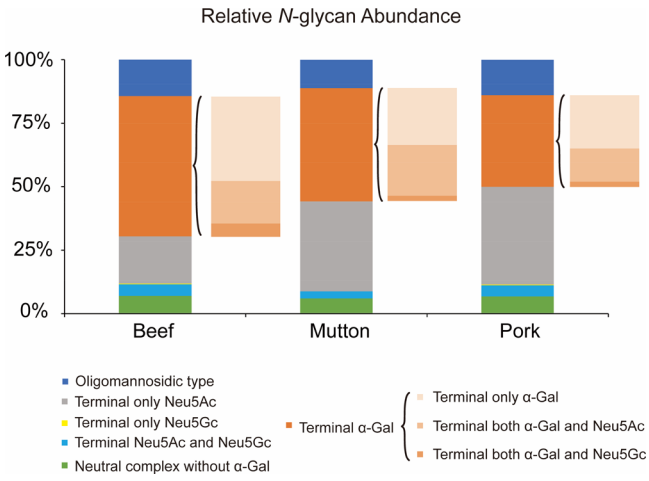

Figure 3. Comparison of the relative abundance of red meat *N*-glycans based on their terminating sugar moiety.

various *N*-glycan types were comparable for all meat species, with average relative abundances of 14.3, 55.4, 18.7, 0.3, 4.6, and 6.8% in beef, 11.2, 44.8, 35.5, 0, 2.7, and 5.8 in mutton, and 14, 36.2, 38.6, 0.3, 4.4, and 6.5% in pork (Supporting Information, Table S4). The highest relative abundance of *N*-glycans with terminal α-Gal motif among the three meat samples was detected in beef, followed by a moderate amount found in mutton and the lowest relative abundance in pork. Furthermore, *N*-glycans with only terminal α-Gal motif represented a great portion of the total α-Gal-containing *N*-glycans, followed by both terminal α-Gal and Neu5Ac, however, the *N*-glycans with both terminal α-Gal and Neu5Gc was only a very low proportion for all meat species. Although CE-ESI-MS/MS analysis was able to identify the α-Gal motif based on signature mass fragments, there is a possibility that in some cases *N*-glycan isomers (i.e., the biantennary H5N4 and H5N4F1 species bearing terminal LacNAc motifs) may co-elute with the α-Gal-containing H5N4 and H5N4F1 and therefore be misattributed to the α-Gal species. Nevertheless, given that the affected *N*-glycan species have a relatively low abundance, attributing them in their entirety to the group of *N*-glycans without the α-Gal motif only slightly reduced the abundance of the rest of *N*-glycans with the terminal α-Gal motif to 49.3% (from 55.4%) in beef, 40.1% (from 44.8%) in mutton, and 31.1% (from 36.2%) in pork, respectively (Supporting Information, Table S4).

Although most *N*-glycan structures were present among the meat samples of the three species, quantitative differences for each structure in the *N*-glycan profile of each species were observed (Supporting Information, Figure S10). In order to achieve a systematic analysis of *N*-glycans, the datasets were pooled together and subjected to principal component analysis (PCA) based on relative abundances of *N*-glycans from beef, mutton, and pork acquired by MALDI-TOF-MS. As shown in the Supporting Information, Figure S11, the obtained dataset was transformed into two principal components (PC1 and PC2). PC1 and PC2 explained 48.4 and 43.5% of variance, respectively. The PCA results can be regarded as reliable by over 90% of the total variance that can be accounted for the two principal components. The resulting score plot, based on the PCA of *N*-glycan profiles of the meat samples, allowed the discrimination of the three tested meat species and the meat sample of each species showed good reproducibility.

Distribution of α-Gal-Containing *N*-Glycans in Beef, Mutton, and Pork Tenderloin. Glycosylation analysis revealed that the majority of *N*-glycans of the analyzed beef, mutton, and pork samples contain the α-Gal motif. To further understand the local distribution as well as the spatial abundance of these *N*-glycans in the meat, MSI was performed on various sections of each species. As shown in Figure 4a, the maltoheptaose DP7 internal standard was distributed in the whole meat tissues, mutton tenderloin generally contained the highest amounts of *N*-glycans, and the α-Gal-containing *N*-glycans were mainly detected at high levels in the perimysial (fibroconnective) surrounding the muscle fascicles (Figure 4b,c). Similar findings were found in a MALDI-MSI analysis of *N*-glycans from pancreas and liver tissues, which also showed higher levels in the fibrous/fibroconnective tissue compared to adjacent regions.[49] A similar spatial distribution for the presence of α-Gal-containing *N*-glycans was reported for porcine heart muscle tissue by using immunohistochemistry.[50] Meat glycoproteins (i.e., collagen, decorin, and fibronectin) are reported to be present in connective tissues, and *N*-glycosylation helps regulate core protein transit, secretion, and cell adhesion.[51−55] Therefore, we hypothesize that these shared *N*-glycan structural motifs across the three meat tissues reflect the glycoproteins carrying them in fibroconnective tissues.

DISCUSSION

The identification of food-derived protein *N*-glycosylation has become increasingly important and has been reported to be a reliable tool in food safety.[26,56,57] Food allergy/sensitivity is one of the most common safety problems, affecting people of all ages and races from all regions.[58] Meat allergies induced by α-Gal following tick bites have only recently been appreciated as a world-wide problem.[59] In-depth, meat glycomics are still limited and mainly based on liquid chromatography−mass spectroscopy (LC−MS) technologies.[26,27] Here, we present a comprehensive overview by analyzing the meat *N*-glycome using MALDI-TOF-MS and CE-ESI-MS, as exemplified by the

https://doi.org/10.1021/acs.jafc.2c08067
J. Agric. Food Chem. 2023, 71, 4184−4192

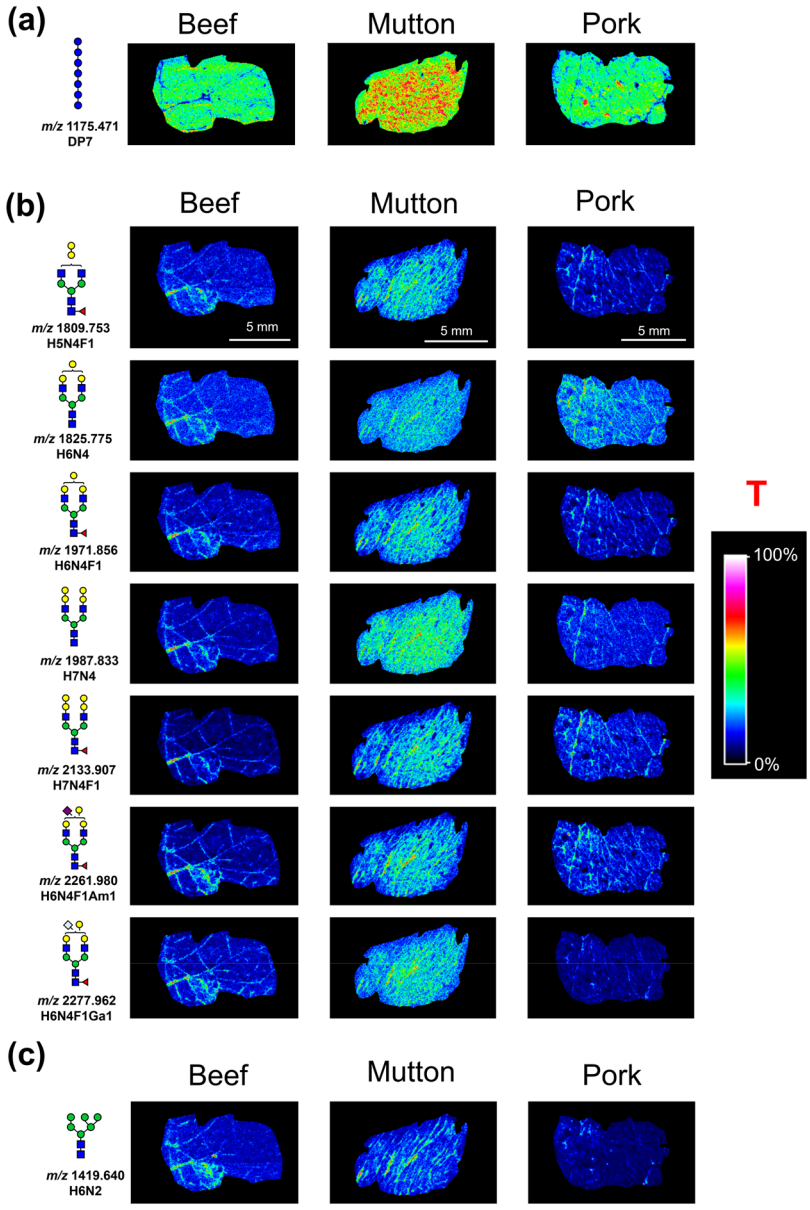

Figure 4. Visualization of maltoheptaose standard (a), terminal α-Gal modified *N*-glycans (b), and H6N2 (c). T = total ion count normalization. For the abbreviations and symbols, refer back to the legend of Figure 2.

identification of 53 and 55 *N*-glycans in beef and pork, respectively, versus the identified 18 and 17 *N*-glycans in a recent study by Chia et al.[27] The similar points with the study by Chia et al. are that we both present a similar level of Neu5Ac-containing *N*-glycans in beef and pork and a much higher level of Neu5Ac-containing *N*-glycans than Neu5Gc-containing *N*-glycans in pork (Supporting Information, Table S5). Interestingly, while the study by Chia et al. reported on high relative abundances of α-Gal-containing *N*-glycans in beef (35.8%) but not in pork (5.1%), our data point to high levels of α-Gal-containing *N*-glycans in both animal species (averages of 55.4% in beef versus 36.2% in pork, Supporting Information, Table S5). Of note, our off-tissue MALDI-TOF-MS data are supported by the MSI data which revealed relative abundances of α-Gal-containing *N*-glycans of approximately 50% in beef and 33% in pork. The possible explanation for the difference between our study and the report by Chia et al.[27] is the use of various analytical platforms (this study used MALDI-TOF-MS, whereas the reported data by Chia et al. used LC−MS analysis[27]) or/and construction of samples (tenderloin in this study versus shank cuts in the study by Chia et al.[27]).

Knowing the distribution of *N*-glycans in meat species not only infers different cell biology aspects about *N*-glycan-related biosynthesis, vesicular transport, or degradation processes but also clearly shows where glycosylated proteins are located, offering the opportunity to further study the effect of glycosylation on meat proteins. The MALDI-MSI analysis of the α-Gal motif in the three meat samples presented herein shows that they are mainly located in the fibroconnective tissues, giving information about its spatial localization and providing guidance on which parts of the meat tissue are less abundant (the actual meat fibers) and which part is highly abundant in *N*-glycans (connective tissues). This knowledge could be used especially for processed meat products, in which only meat fibers are required as a functional ingredient (i.e., for certain sausages or canned meat). Separation of the

https://doi.org/10.1021/acs.jafc.2c08067
J. Agric. Food Chem. 2023, 71, 4184−4192

extracellular matrix would make these meat products virtually α-Gal-free. Some proteins from connective tissues were reported to undergo *N*-glycosylation;[52,54,55] even though the role of glycosylation has not been fully elucidated, it is speculated that glycosylation is related to the directional arrangement of fibroconnective tissues.[53] In addition, although our study shows similar results to those of other related studies,[34,49] it is worth pointing out that the construction may differ between fibroconnective tissues and other tissues; therefore, the release efficiency difference by PNGase F on fibroconnective tissues and other tissues should be considered.

The herein analysis on the identification and spatial distribution of α-Gal-containing *N*-glycans in three meat samples may promote a deeper understanding on meat glycosylation and also provide theoretical guidance for processed meat products. However, the herein analyzed meat samples for each species were limited to tenderloin cuts; therefore, the herein presented relative abundance of *N*-glycans from other beef, mutton, and pork cuts may vary. Furthermore, the meat tissues used in this study were only from one cut type (tenderloin part). As glycosylation varies significantly between various organs of the same animal, potential differences in the *N*-glycan profile of various muscle tissues may also be possible[60] and should be further investigated. The application of this herein presented methodology to analyze the spatial organization of *N*-glycans of various types of animal offal is part of our current research endeavor.

■ ASSOCIATED CONTENT

Supporting Information

The Supporting Information is available free of charge at https://pubs.acs.org/doi/10.1021/acs.jafc.2c08067.

Overview of *N*-glycan sample preparation for MS analysis; MALDI-MSI workflow for beef, mutton, and pork tenderloin *N*-glycan analysis; extracted ion electropherograms of typical *N*-glycans from meat samples; CE-ESI-MS/MS fragmentation spectra of GirP labeled beef *N*-glycans; CE-ESI-MS/MS fragmentation spectra of GirP labeled mutton *N*-glycans; CE-ESI-MS/MS fragmentation spectra of GirP-labeled pork *N*-glycans; PNGase F released beef tenderloin *N*-glycans analyzed by MALDI-TOF-MS; PNGase F released mutton tenderloin *N*-glycans analyzed by MALDI-TOF-MS; PNGase F released pork tenderloin *N*-glycans analyzed by MALDI-TOF-MS; differentiation analysis of beef, mutton, and pork tenderloin *N*-glycans; Figure S11, and principal component analysis of relative abundances of *N*-glycans of beef, mutton, and pork (PDF)

Beef *N*-glycans identified with MALDI-TOF-MS and CE-ESI-MS(/MS); mutton *N*-glycans identified with MALDI-TOF-MS and CE-ESI-MS(/MS); pork *N*-glycans identified with MALDI-TOF-MS and CE-ESI-MS(/MS); relative abundances of the various *N*-glycan types for beef, mutton, and pork; and relative abundance of α-Gal, Neu5Ac, and Neu5Gc in *N*-glycans of beef, mutton, and pork (XLSX)

■ AUTHOR INFORMATION

Corresponding Authors

Li Liu − *Glycomics and Glycan Bioengineering Research Center (GGBRC), College of Food Science and Technology, Nanjing Agricultural University, Nanjing 210095, China;* orcid.org/0000-0002-2178-9237; Email: lichen.liu@njau.edu.cn

Bram Heijs − *Center for Proteomics and Metabolomics, Leiden University Medical Center, Leiden 2333 ZA, The Netherlands;* orcid.org/0000-0001-6328-9305; Email: b.p.a.m.heijs@lumc.nl

Josef Voglmeir − *Glycomics and Glycan Bioengineering Research Center (GGBRC), College of Food Science and Technology, Nanjing Agricultural University, Nanjing 210095, China;* orcid.org/0000-0002-4096-4926; Email: josef.voglmeir@njau.edu.cn

Authors

Rui-Rui Guo − *Glycomics and Glycan Bioengineering Research Center (GGBRC), College of Food Science and Technology, Nanjing Agricultural University, Nanjing 210095, China; Center for Proteomics and Metabolomics, Leiden University Medical Center, Leiden 2333 ZA, The Netherlands*

Guinevere S. M. Lageveen-Kammeijer − *Center for Proteomics and Metabolomics, Leiden University Medical Center, Leiden 2333 ZA, The Netherlands;* orcid.org/0000-0001-7670-1151

Wenjun Wang − *Center for Proteomics and Metabolomics, Leiden University Medical Center, Leiden 2333 ZA, The Netherlands*

Hans Dalebout − *Center for Proteomics and Metabolomics, Leiden University Medical Center, Leiden 2333 ZA, The Netherlands*

Wangang Zhang − *National Center of Meat Quality and Safety Control, College of Food Science and Technology, Nanjing Agricultural University, Nanjing 210095, China;* orcid.org/0000-0001-6910-130X

Manfred Wuhrer − *Center for Proteomics and Metabolomics, Leiden University Medical Center, Leiden 2333 ZA, The Netherlands;* orcid.org/0000-0002-0814-4995

Complete contact information is available at: https://pubs.acs.org/10.1021/acs.jafc.2c08067

Funding

This study was supported by the China Scholarship Council (202006850033 to R.R.G., 201607720041 to W.J.W.) and in parts by the National Natural Science Foundation of China (grant numbers 31471703, 31671854, 31871793, and 31871754 to J.V. and L.L.), and the 100 Foreign Talents Plan (grant number JSB2014012 to J.V.).

Notes

The authors declare no competing financial interest.

■ ABBREVIATIONS

α-Gal, galactose-α-1,3-galactose; MALDI-TOF-MS, matrix-assisted laser desorption/ionization time-of-flight mass spectrometry; MALDI-MSI, matrix-assisted laser desorption/ionization mass spectrometry imaging; CE-ESI-MS, capillary electrophoresis hyphenated with mass spectrometry via electrospray ionization; IgE, immunoglobulin E; α1,3GT, α-1,3-galactosyltransferase; HAc, glacial acetic acid; EtOH, ethanol; DMSO, dimethylsulfoxide; HoBt, 1-hydroxybenzotriazole hydrate; CHCA, α-cyano-4-hydroxycinnamic acid; TFA, trifluoroacetic acid; DP7, maltoheptaose; EDC, 1-ethyl-3-(3-dimethylaminopropyl)carbodiimide; ACN, acetonitrile; GirP, 1-(hydrazinocarbonylmethyl)pyridinium chloride; ITO, indium-tin-oxide; HILIC, hydrophilic interaction liquid

chromatography; IPQ, isotopic pattern quality; BGE, background electrolyte

REFERENCES

(1) Van Nunen, S. A.; O'Connor, K. S.; Clarke, L. R.; Boyle, R. X.; Fernando, S. L. An association between tick bite reactions and red meat allergy in humans. *Med. J. Aust.* **2009**, *190*, 510−511.

(2) Rappo, T. B.; Cottee, A. M.; Ratchford, A. M.; Burns, B. J. Tick bite anaphylaxis: Incidence and management in an australian emergency department. *Emerg. Med. Australas.* **2013**, *25*, 297−301.

(3) Mateos-Hernández, L.; Villar, M.; Moral, A.; Rodríguez, C. G.; Arias, T. A.; de la Osa, V.; Brito, F. F.; Fernández de Mera, I. G.; Alberdi, P.; Ruiz-Fons, F.; Cabezas-Cruz, A.; Estrada-Peña, A.; de la Fuente, J. Tick-host conflict: Immunoglobulin e antibodies to tick proteins in patients with anaphylaxis to tick bite. *Oncotarget* **2017**, *8*, 20630−20644.

(4) Kiewiet, M. B. G.; Apostolovic, D.; Starkhammar, M.; Grundström, J.; Hamsten, C.; van Hage, M. Clinical and serological characterization of the α-gal syndrome—importance of atopy for symptom severity in a european cohort. *J. Allergy Clin. Immunol. Pract.* **2020**, *8*, 2027−2034.

(5) Araujo, R. N.; Franco, P. F.; Rodrigues, H.; Santos, L. C. B.; McKay, C. S.; Sanhueza, C. A.; Brito, C. R. N.; Azevedo, M. A.; Venuto, A. P.; Cowan, P. J.; Almeida, I. C.; Finn, M. G.; Marques, A. F. Amblyomma sculptum tick saliva: A-gal identification, antibody response and possible association with red meat allergy in brazil. *Int. J. Parasitol.* **2016**, *46*, 213−220.

(6) Wen, L.; Zhou, J.; Yin, J.; Sun, J.-L.; Sun, Y.; Wu, K.; Katial, R. Delayed anaphylaxis to red meat associated with specific ige antibodies to galactose. *J. Allergy Clin. Immunol.* **2015**, *7*, 92−94.

(7) Commins, S. P.; Satinover, S. M.; Hosen, J.; Mozena, J.; Borish, L.; Lewis, B. D.; Woodfolk, J. A.; Platts-Mills, T. A. Delayed anaphylaxis, angioedema, or urticaria after consumption of red meat in patients with ige antibodies specific for galactose-alpha-1,3-galactose. *J. Allergy Clin. Immunol. Pract.* **2009**, *123*, 426−433.

(8) Apostolovic, D.; Tran, T. A. T.; Sánchez-Vidaurre, S.; Cirkovic Velickovic, T.; Starkhammar, M.; Hamsten, C.; van Hage, M. Red meat allergic patients have a selective ige response to the α-gal glycan. *Allergy* **2015**, *70*, 1497−1500.

(9) Jacquenet, S.; Moneret-Vautrin, D. A.; Bihain, B. E. Mammalian meat-induced anaphylaxis: Clinical relevance of anti-galactose-alpha-1,3-galactose ige confirmed by means of skin tests to cetuximab. *J. Allergy Clin. Immunol. Pract.* **2009**, *124*, 603−605.

(10) Bircher, A.; Hofmeier, K.; Link, S.; Heijnen, I. Food allergy to the carbohydrate galactose-alpha-1,3-galactose (alpha-gal): Four case reports and a review. *Eur. J. Dermatol.* **2017**, *27*, 3−9.

(11) Maruyama, S.; Cantu 3rd, E.; Galili, U.; D'Agati, V.; Godman, G.; Stern, D. M.; Andres, G. Alpha-galactosyl epitopes on glycoproteins of porcine renal extracellular matrix. *Kidney Int.* **2000**, *57*, 655−663.

(12) Galili, U.; Shohet, S. B.; Kobrin, E.; Stults, C. L.; Macher, B. A. Man, apes, and old world monkeys differ from other mammals in the expression of alpha-galactosyl epitopes on nucleated cells. *J. Biol. Chem.* **1988**, *263*, 17755−17762.

(13) Langley, D. B.; Schofield, P.; Nevoltris, D.; Jackson, J.; Jackson, K. J. L.; Peters, T. J.; Burk, M.; Matthews, J. M.; Basten, A.; Goodnow, C. C.; van Nunen, S.; Reed, J. H.; Christ, D. Genetic and structural basis of the human anti-α-galactosyl antibody response. *Proc. Natl. Acad. Sci. U. S. A.* **2022**, *119*, No. e2123212119.

(14) de la Fuente, J.; Cabezas-Cruz, A.; Pacheco, I. Alpha-gal syndrome: Challenges to understanding sensitization and clinical reactions to alpha-gal. *Expert Rev. Mol. Diagn.* **2020**, *20*, 905−911.

(15) Galili, U. Evolution in primates by "catastrophic-selection" interplay between enveloped virus epidemics, mutated genes of enzymes synthesizing carbohydrate antigens, and natural anti-carbohydrate antibodies. *Am. J. Phys. Anthropol.* **2019**, *168*, 352−363.

(16) Sharma, S. R.; Karim, S. Tick saliva and the alpha-gal syndrome: Finding a needle in a haystack. *Front. Cell. Infect. Microbiol.* **2021**, *11*, No. 680264.

(17) Villar, M.; Pacheco, I.; Mateos-Hernández, L.; Cabezas-Cruz, A.; Tabor, A. E.; Rodríguez-Valle, M.; Mulenga, A.; Kocan, K. M.; Blouin, E. F.; de La Fuente, J. Characterization of tick salivary gland and saliva alphagalactome reveals candidate alpha-gal syndrome disease biomarkers. *Expert Rev. Proteomics* **2021**, *18*, 1099−1116.

(18) Román-Carrasco, P.; Hemmer, W.; Cabezas-Cruz, A.; Hodžić, A.; de la Fuente, J.; Swoboda, I. The α-gal syndrome and potential mechanisms. *Front. Allergy* **2021**, *2*, No. 783279.

(19) Knight, M.; Wyatt, K.; James, H. Exercise-induced anaphylaxis after consumption of red meat in a patient with ige antibodies specific for galactose-alpha-1,3-galactose. *J. Allergy Clin. Immunol. Pract.* **2015**, *3*, 801−802.

(20) Commins, S. P. Diagnosis & management of alpha-gal syndrome: Lessons from 2,500 patients. *Expert Rev. Clin. Immunol.* **2020**, *16*, 667−677.

(21) Ma, Y.; Hou, Y.; Xie, K.; Zhang, L.; Zhou, P. Digestive differences in immunoglobulin g and lactoferrin among human, bovine, and caprine milk following in vitro digestion. *Int. Dairy J.* **2021**, *120*, No. 105081.

(22) Wang, B.; Timilsena, Y. P.; Blanch, E.; Adhikari, B. Lactoferrin: Structure, function, denaturation and digestion. *Crit. Rev. Food Sci. Nutr.* **2019**, *59*, 580−596.

(23) van der Kraan, M. I.; Groenink, J.; Nazmi, K.; Veerman, E. C.; Bolscher, J. G.; Nieuw Amerongen, A. V. Lactoferrampin: A novel antimicrobial peptide in the n1-domain of bovine lactoferrin. *Peptides* **2004**, *25*, 177−183.

(24) Demers-Mathieu, V.; Underwood, M. A.; Beverly, R. L.; Nielsen, S. D.; Dallas, D. C. Comparison of human milk immunoglobulin survival during gastric digestion between preterm and term infants. *Nutrients* **2018**, *10*, 631.

(25) Chung, Y. C.; Kim, Y. S.; Shadchehr, A.; Garrido, A.; Macgregor, I. L.; Sleisenger, M. H. Protein digestion and absorption in human small intestine. *Gastroenterology* **1979**, *76*, 1415−1421.

(26) Shi, Z.; Yin, B.; Yuquan, L.; Zhou, G. H.; Li, C.; Xu, X.-L.; Luo, X.; Zhang, X.; Voglmeir, J.; Liu, L. N-glycan profile as a tool in qualitative and quantitative analysis of meat adulteration. *J. Agric. Food Chem.* **2019**, *67*, 10543−10551.

(27) Chia, S.; Teo, G.; Tay, S. J.; Loo, L. S. W.; Wan, C.; Sim, L. C.; Yu, H.; Walsh, I.; Pang, K. T. An integrative glycomic approach for quantitative meat species profiling. *Foods* **2022**, *11*, 1952.

(28) Ma, X.; Fernández, F. M. Advances in mass spectrometry imaging for spatial cancer metabolomics. *Mass Spectrom. Rev.* **2022**, No. e21804.

(29) Sgobba, E.; Daguerre, Y.; Giampà, M. Unravel the local complexity of biological environments by maldi mass spectrometry imaging. *Int. J. Mol. Sci.* **2021**, *22*, 12393.

(30) Schnackenberg, L. K.; Thorn, D. A.; Barnette, D.; Jones, E. E. Maldi imaging mass spectrometry: An emerging tool in neurology. *Metab. Brain Dis.* **2022**, *37*, 105−121.

(31) Kip, A. M.; Valverde, J. M.; Altelaar, M.; Heeren, R. M. A.; Hundscheid, I. H. R.; Dejong, C. H. C.; Olde Damink, S. W. M.; Balluff, B.; Lenaerts, K. Combined quantitative (phospho)proteomics and mass spectrometry imaging reveal temporal and spatial protein changes in human intestinal ischemia-reperfusion. *J. Proteome Res.* **2022**, *21*, 49−66.

(32) Loch, F. N.; Klein, O.; Beyer, K.; Klauschen, F.; Schineis, C.; Lauscher, J. C.; Margonis, G. A.; Degro, C. E.; Rayya, W.; Kamphues, C. Peptide signatures for prognostic markers of pancreatic cancer by maldi mass spectrometry imaging. *Biology* **2021**, *10*, 1033.

(33) Fincher, J. A.; Djambazova, K. V.; Klein, D. R.; Dufresne, M.; Migas, L. G.; Van de Plas, R.; Caprioli, R. M.; Spraggins, J. M. Molecular mapping of neutral lipids using silicon nanopost arrays and tims imaging mass spectrometry. *J. Am. Soc. Mass Spectrom.* **2021**, *32*, 2519−2527.

(34) Wang, Z.; Fu, W.; Huo, M.; He, B.; Liu, Y.; Tian, L.; Li, W.; Zhou, Z.; Wang, B.; Xia, J.; Chen, Y.; Wei, J.; Abliz, Z. Spatial-resolved metabolomics reveals tissue-specific metabolic reprogramming in diabetic nephropathy by using mass spectrometry imaging. *Acta Pharm. Sin. B* **2021**, *11*, 3665−3677.

https://doi.org/10.1021/acs.jafc.2c08067
J. Agric. Food Chem. 2023, 71, 4184−4192

(35) Powers, T. W.; Jones, E. E.; Betesh, L. R.; Romano, P. R.; Gao, P.; Copland, J. A.; Mehta, A. S.; Drake, R. R. Matrix assisted laser desorption ionization imaging mass spectrometry workflow for spatial profiling analysis of n-linked glycan expression in tissues. *Anal. Chem.* **2013**, *85*, 9799−9806.
(36) Drake, R. R.; McDowell, C.; West, C.; David, F.; Powers, T. W.; Nowling, T.; Bruner, E.; Mehta, A. S.; Angel, P. M.; Marlow, L. A.; Tun, H. W.; Copland, J. A. Defining the human kidney n-glycome in normal and cancer tissues using maldi imaging mass spectrometry. *J. Mass Spectrom.* **2020**, *55*, No. e4490.
(37) West, C. A.; Wang, M.; Herrera, H.; Liang, H.; Black, A.; Angel, P. M.; Drake, R. R.; Mehta, A. S. N-linked glycan branching and fucosylation are increased directly in hcc tissue as determined through in situ glycan imaging. *J. Proteome Res.* **2018**, *17*, 3454−3462.
(38) Veličković, D.; Liao, Y.-C.; Thibert, S.; Veličković, M.; Anderton, C.; Voglmeir, J.; Stacey, G.; Zhou, M. Spatial mapping of plant n-glycosylation cellular heterogeneity inside soybean root nodules provided insights into legume-rhizobia symbiosis. *Front. Plant Sci.* **2022**, *13*, No. 869281.
(39) Boyaval, F.; van Zeijl, R.; Dalebout, H.; Holst, S.; van Pelt, G.; Fariña-Sarasqueta, A.; Mesker, W.; Tollenaar, R.; Morreau, H.; Wuhrer, M.; Heijs, B. N-glycomic signature of stage ii colorectal cancer and its association with the tumor microenvironment. *Mol. Cell. Proteomics* **2021**, *20*, 100057.
(40) Boyaval, F.; Dalebout, H.; Van Zeijl, R.; Wang, W.; Fariña-Sarasqueta, A.; Lageveen-Kammeijer, G. S. M.; Boonstra, J. J.; McDonnell, L. A.; Wuhrer, M.; Morreau, H.; Heijs, B. High-mannose n-glycans as malignant progression markers in early-stage colorectal cancer. *Cancers* **2022**, *14*, 1552.
(41) Enomoto, H.; Kotani, M.; Ohmura, T. Novel blotting method for mass spectrometry imaging of metabolites in strawberry fruit by desorption/ionization using through hole alumina membrane. *Foods* **2020**, *9*, 408−415.
(42) Franceschi, P.; Dong, Y.; Strupat, K.; Vrhovsek, U.; Mattivi, F. Combining intensity correlation analysis and maldi imaging to study the distribution of flavonols and dihydrochalcones in golden delicious apples. *J. Exp. Bot.* **2012**, *63*, 1123−1133.
(43) Lageveen-Kammeijer, G. S. M.; de Haan, N.; Mohaupt, P.; Wagt, S.; Filius, M.; Nouta, J.; Falck, D.; Wuhrer, M. Highly sensitive ce-esi-ms analysis of n-glycans from complex biological samples. *Nat. Commun.* **2019**, *10*, 2137.
(44) Selman, M. H. J.; Hemayatkar, M.; Deelder, A. M.; Wuhrer, M. Cotton hilic spe microtips for microscale purification and enrichment of glycans and glycopeptides. *Anal. Chem.* **2011**, *83*, 2492−2499.
(45) Jansen, B. C.; Reiding, K. R.; Bondt, A.; Hipgrave Ederveen, A. L.; Palmblad, M.; Falck, D.; Wuhrer, M. Massytools: A high-throughput targeted data processing tool for relative quantitation and quality control developed for glycomic and glycoproteomic maldi-ms. *J. Proteome Res.* **2015**, *14*, 5088−5098.
(46) Kammeijer, G. S. M.; Kohler, I.; Jansen, B. C.; Hensbergen, P. J.; Mayboroda, O. A.; Falck, D.; Wuhrer, M. Dopant enriched nitrogen gas combined with sheathless capillary electrophoresis−electrospray ionization-mass spectrometry for improved sensitivity and repeatability in glycopeptide analysis. *Anal. Chem.* **2016**, *88*, 5849−5856.
(47) Holst, S.; Heijs, B.; de Haan, N.; van Zeijl, R. J. M.; Briaire-de Bruijn, I. H.; van Pelt, G. W.; Mehta, A. S.; Angel, P. M.; Mesker, W. E.; Tollenaar, R. A.; Drake, R. R.; Bovée, J. V. M. G.; McDonnell, L. A.; Wuhrer, M. Linkage-specific in situ sialic acid derivatization for n-glycan mass spectrometry imaging of formalin-fixed paraffin-embedded tissues. *Anal. Chem.* **2016**, *88*, 5904−5913.
(48) Ghirardello, M.; Zhang, Y.-Y.; Voglmeir, J.; Galan, M. C. Recent applications of ionic liquid-based tags in glycoscience. *Carbohydr. Res.* **2022**, *520*, No. 108643.
(49) Powers, T. W.; Holst, S.; Wuhrer, M.; Mehta, A. S.; Drake, R. R. Two-dimensional n-glycan distribution mapping of hepatocellular carcinoma tissues by maldi-imaging mass spectrometry. *Biomolecules* **2015**, *5*, 2554−2572.
(50) Wang, R. G.; Ruan, M.; Zhang, R. J.; Chen, L.; Li, X. X.; Fang, B.; Li, C.; Ren, X. Y.; Liu, J. Y.; Xiong, Q.; Zhang, L. N.; Jin, Y.; Li, L.; Li, R.; Wang, Y.; Yang, H. Y.; Dai, Y. F. Antigenicity of tissues and organs from ggta1/cmah/β4galnt2 triple gene knockout pigs. *J. Biomed. Res.* **2018**, *33*, 235−243.
(51) Klein, J. A.; Meng, L.; Zaia, J. Deep sequencing of complex proteoglycans: A novel strategy for high coverage and site-specific identification of glycosaminoglycan-linked peptides. *Mol. Cell. Proteomics* **2018**, *17*, 1578−1590.
(52) Seo, N. S.; Hocking, A. M.; Hök, M.; McQuillan, D. J. Decorin core protein secretion is regulated by n-linked oligosaccharide and glycosaminoglycan additions. *J. Biol. Chem.* **2005**, *280*, 42774−42784.
(53) Ushiki, T. Collagen fibers, reticular fibers and elastic fibers. A comprehensive understanding from a morphological viewpoint. *Arch. Histol. Cytol.* **2002**, *65*, 109−126.
(54) Boyd, A.; Montandon, M.; Wood, A. J.; Currie, P. D. Fkrp directed fibronectin glycosylation: A novel mechanism giving insights into muscular dystrophies? *BioEssays* **2022**, *44*, No. e2100270.
(55) Jürgensen, H. J.; Madsen, D. H.; Ingvarsen, S.; Melander, M. C.; Gårdsvoll, H.; Patthy, L.; Engelholm, L. H.; Behrendt, N. A novel functional role of collagen glycosylation: Interaction with the endocytic collagen receptor uparap/endo180*. *J. Biol. Chem.* **2011**, *286*, 32736−32748.
(56) Wang, T.; Hu, X.-C.; Cai, Z.-P.; Voglmeir, J.; Liu, L. Qualitative and quantitative analysis of carbohydrate modification on glycoproteins from seeds of ginkgo biloba. *J. Agric. Food Chem.* **2017**, *65*, 7669−7679.
(57) Tang, W.; Liu, D.; Nie, S.-P. Food glycomics in food science: Recent advances and future perspectives. *Curr. Opin. Food Sci.* **2022**, *46*, No. 100850.
(58) Boye, J. I. Food allergies in developing and emerging economies: Need for comprehensive data on prevalence rates. *Clin. Transl. Allergy* **2012**, *2*, 25.
(59) van Nunen, S. Tick-induced allergies: Mammalian meat allergy, tick anaphylaxis and their significance. *Asia Pac. Allergy* **2015**, *5*, 3−16.
(60) Jahan, M.; Thomson, P. C.; Wynn, P. C.; Wang, B. The non-human glycan, n-glycolylneuraminic acid (neu5gc), is not expressed in all organs and skeletal muscles of nine animal species. *Food Chem.* **2021**, *343*, No. 128439.

https://doi.org/10.1021/acs.jafc.2c08067
J. Agric. Food Chem. 2023, 71, 4184−4192